Memory-based Jitter: Improving Visual Recognition on Long-tailed Data with Diversity In Memory

Jialun Liu[1]*, **Jingwei Zhang**[2]*, **Wenhui Li**[1]†, **Chi Zhang**[3] **Yifan Sun**[3]
[1] Jilin University [2] Tsinghua University [3] Megvii Inc.
jialun18@mails.jlu.edu.cn zjw18@mails.tsinghua.edu.cn
liwh@jlu.edu.cn peter@megvii.co

Abstract

This paper considers deep visual recognition on long-tailed data, with the majority categories only occupying relatively few samples. The tail categories are prone to lack of within-class diversity, which compromises the representative ability of the learned visual concepts. A radical solution is to augment the tail categories with higher diversity. To this end, we introduce a simple and reliable method named Memory-based Jitter (MBJ) to gain extra diversity for the tail data. We observe that the deep model keeps on jittering from one historical edition to another, even when it already approaches convergence. The "jitter" means the small variations between historical models. We argue that such jitter largely originates from the within-class diversity of the overall data and thus encodes the within-class distribution pattern. To utilize such jitter for tail data augmentation, we store the jitter among historical models into a memory bank and get the so-called Memory-based Jitter. With slight modifications, MBJ is applicable for two fundamental visual recognition tasks, *i.e.*, image classification and deep metric learning (on long-tailed data). On image classification, MBJ collects the historical embeddings to learn an accurate classifier. In contrast, on deep metric learning, it collects the historical prototypes of each class to learn a robust deep embedding. Under both scenarios, MBJ enforces higher concentration on tail classes, so as to compensate for their lack of diversity. Extensive experiments on three long-tailed classification benchmarks and two deep metric learning benchmarks (person re-identification, in particular) demonstrate the significant improvement. Moreover, the achieved performance are on par with the state-of-the-art on both tasks.

1 Introduction

In visual recognition tasks, the long-tailed distribution of the data is a common and natural problem under realistic scenarios [35, 18, 8, 10]. A few categories (*i.e.*, the head classes) occupy most of the data while the most categories (*i.e.*, the tail classes) only occupy relatively few data. Such long-tailed distribution significantly challenges deep visual recognition, including both image classification [46, 14, 5, 35, 2, 6, 48] and deep metric learning [19, 42, 10, 32]. To be general, this paper considers long-tailed visual recognition on these two elemental tasks with a uniform motivation.

We recognize the insufficient within-class diversity of the tail classes as the most prominent reason that hinders long-tailed deep visual recognition. Given various images of a same class, a deep model basically maps them into a compact cluster in deep embedding space, yielding a corresponding visual concept.

*Equal contribution.
†Corresponding author.

Preprint. Under review.

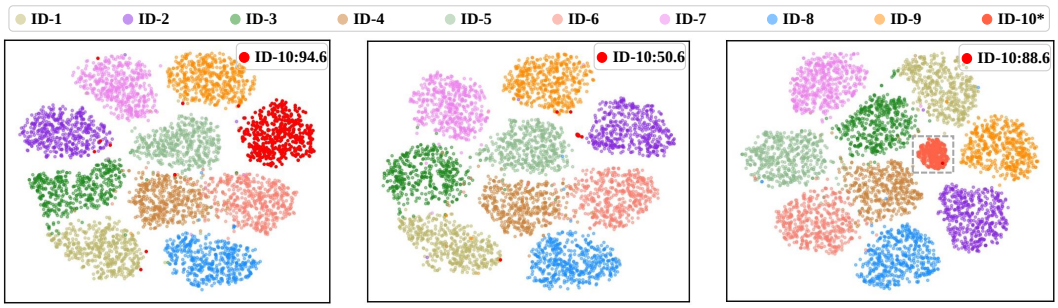

(a) (b) (c)

Figure 1: Visualization of the feature distribution on CIFAR-10 with t-SNE. When a specified class ("ID-10") degrades from head (a) to tail (b), its visual concept corrupts to a very limited scope in the deep embedding. The classification accuracy dramatically decreases from 94.6% to 50.6%. In (c), MBJ collects historical tail features (ID-10*) into a memory bank to augment the tail class. The historical tail features significantly enrich the corresponding within-class diversity. Accordingly, the classification accuracy increases from 50.6% to 88.6%.

Since the tail classes have very limited amount of training samples, the learned visual concepts are not representative, which deteriorates the recognition accuracy. To better illustrate this point, we visualize the deep embedding of CIFAR-10 in Fig. 1. When a specified class ("ID-10") degrades from head (Fig. 1(a)) to tail (Fig. 1(b)), its visual concept reduces to a very limited scope in the embedding space. Consequentially, when we employ the model for inference, samples from "ID-10" may exceed the already-learned scope and are thus easily mis-classified. Intuitively, a radical solution is to augment the tail classes with higher diversity.

During the seek for additional diversity, we notice the jittering phenomenon of deep model, which means the small variations between historical models, and find it informative. Specifically, the deep model keeps on jittering from one edition to another as the training progresses, even when it already approaches convergence. The phenomenon is consistent with the observation in many literature [40, 16, 31]. Contrary to their attempt to avoid or suppress the model jitters (as to be discussed in Section 2 in details), we consider that these jitters are informative. Experimental investigation shows that such jitters largely originate from the within-class diversity of the overall data, because increasing the training data per class usually enlarges the jittering amplitude (as to be detailed in Section 3.1). We thus infer that the model jitters encode the within-class diversity and offer clues to augment the tail data.

With the above insight, we propose Memory-based Jitter (MBJ) for long-tailed visual recognition. MBJ collects the jitters among historical models, iteration by iteration, and stores them into a memory bank, yielding the so-called Memory-based Jitter. With slight modifications, MBJ is capable to accommodate two elemental visual recognition tasks. On image classification, MBJ collects the historical embeddings with higher concentration on tail classes. Correspondingly, it significantly enriches the tail diversity (as shown in Fig. 1(c)), enhances the corresponding representative ability and increases classification accuracy. In contrast, on deep metric learning, MBJ collects the historical prototypes (*i.e.*, the weight vectors in the classification layer). The multiple prototypes jointly supervise the tail samples, which promotes better generalization ability of the learned embedding.

We note that MBJ is also featured for a novel re-balancing strategy. To enforce higher concentration on the tail classes, MBJ abandons the common practices of re-sampling the raw images (which has been evidenced as compromising deep embedding learning [46, 14]) or re-weighting the classes [6, 13, 41]. Instead, MBJ re-samples the historical features / prototypes from memory and maintains natural probabilities for sampling the raw images. The detailed differences between MBJ and prior methods *w.r.t.* re-balancing strategy are discussed in Section 2.

The main contributions of this paper are summarized as follows:

- We find that the model jitters are informative. They encode the within-class diversity of the overall data and offer reliable resources to gain extra diversity for tail data augmentation.

- We propose Memory-based Jitter to improve deep visual recognition on long-tailed data. MBJ is compatible to two elemental visual tasks, *i.e.*, image classification and deep metric learning, with slight modifications.
- We conduct extensive experiments on three classification benchmarks and two person re-identification benchmarks under long-tailed scenario. On all these benchmarks, we demonstrate the superiority of our methods with significant improvement over the baseline, as well as state-of-the-art performance.

2 Related work

Re-balancing strategy matters for long-tailed classification. Since the tail classes have relatively few samples, it is intuitive to highlight them during training. To this end, there are two popular re-balancing strategies, *i.e.*, *re-weighting*[13, 41, 6] and *re-sampling*[25, 45, 3, 4]. Re-weighting strategy allocates larger weights to tail classes in loss function. Re-sampling over-samples the raw images of the tail classes for training. Some recent works rethink these strategies and make further improvement. For example, re-weighting strategy provides no diversity for the tail classes. [46, 14] find that re-sampling the raw images actually compromises the deep embedding, in spite of the overall improvement.

In comparison, the re-balancing strategy of our method is novel. To highlight the tail classes, MBJ re-samples the memory, rather than the raw images. The advantages are two-fold. On the one hand, it naturally decouples the operations of sampling the raw images and highlighting the tail classes. It thus avoids the potential deterioration to the deep embedding [46, 14]. On the other hand, with continuing jitters, the re-sampled memory explicitly provides extra diversity for the tail data. Combining these two advantages, MBJ significantly improves long-tailed visual recognition.

Memory-based learning has been explored in several computer vision domains [11, 31, 16, 40, 24, 47]. In unsupervised learning, [11] employs memory to include more data in the dictionary. It shows that larger optimization scope within a optimization step is beneficial for unsupervised learning [11]. In semi-supervised learning, [16, 31] enforce consistency between historical predictions. Such consistency offers auxiliary supervision for the unlabeled data. In supervised deep metric learning, [40] uses memory to enhance the hard mining effect. Regardless of their objectives of using memory, they all hold a negative attitude towards the jitters. [11] and [16, 31] suppress the jitters with momentum and consistency constraint, respectively. [40] tries to avoid the jitters by delaying the injection of memory.

In contrast to their negative attitude towards jitters, we find that the jitters are informative and provide clues to substantially augment the tail classes. As a major contribution of this work, we analyze the mechanism in Section 3.1 and experimentally validate its effectiveness in Section 4.

Moreover, we notice a recent work IEM [48] also employs memory for long-tailed image classification. We compare MBJ against IEM in details for clarity.Our method significantly differs from IEM in three aspects, *i.e.*, the applied task, the mechanism and the achieved performance. First, IEM is specified for image classification, while MBJ improves both image classification and deep metric learning with a uniform motivation. Second, IEM considers tail classes are harder to recognize, and thus employ more prototypes from the memory for higher redundancy, while MBJ employs the jitters in memory to augment the diversity of tail data. Finally, on image classification task, MBJ maintains competitive performance with significantly higher computing efficiency. IEM requires extraordinary large amount of memory (up to 50000 per class), and achieves an error rate of 33% on iNaturelist. In contrast, MBJ only stores 25000 memorized features in total and achieves an error rate of 31.36% (-1.64% error) on iNaturelist18 [34].

3 Proposed Method

3.1 Informative Jitters

We first analyze the cause of model jitters and explain why it is informative for tail data augmentation.

First, given the abundant training data, model jitters are inevitable. The optimization of deep learning is based on the Stochastic Gradient Decent (SGD) [1]. To learn from the abundant data,

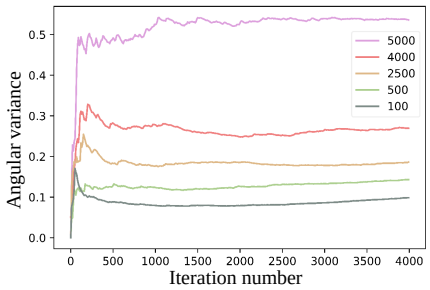

Figure 2: The change of jittering amplitude during training in different amount of training data. We change the number of samples per head class (from 5000 to 100) to control the diversity degree. The ordinate represents the angular variance between historical features of one instance, which indicates the jittering amplitude. The abscissa represents the iteration number during training.

SGD divides the whole data into several minibatches, and updates the model iteratively. It thus inevitably (slightly) biases the model to the current minibatch, resulting in jitters from one iteration to the next. *Second, the data between neighboring minibatches present within-class diversity (as well as some degree of inter-class diversity)*, because samples from a same class are scattered among several minibatches. These two factors jointly endow the model jitters with information encoded from within-class diversity.

To validate the above hypothesis, we experimentally investigate the impact of the diversity degree on the jitter amplitude. We conduct the toy experiment on CIFAR-10 [15, 33]. We set a specified class as the tail class and observe the jitter of a single tail sample. Since the samples are transformed into a feature vector in the deep embedding, we calculate the geometrical angular variance between historical features to indicate the jitter amplitude. We change the number of samples per head class (from 5000 to 100) to control the diversity degree. The jitter amplitudes corresponding to different data diversity degrees are shown in Fig. 2, from which we draw three observations.

First, we observe a clear jitter phenomenon under all the settings. We note that the model has already approached convergence during this observation. It confirms our argument about the existence of the model jitter. Second, the data diversity directly impacts the jitter amplitude. Larger amount of samples per (head) classes incurs larger jitter to a single sample of the tail class. It validates that the the model jitter largely originates from the overall within-class diversity. Third, the jitters need accumulation over several iterations to reach a stable level. It thus motivates us to store the model jitters with memory bank.

Based on the above observations and arguments, we propose Memory-based Jitter module to utilize the jitter for tail data augmentation. MBJ is simple yet effective. With a slight modification, it is capable to accommodate both image classification and deep metric learning tasks.

3.2 Image classification

On image classification, MBJ module stores the features in current mini-batch to form a feature memory as shown in Fig.3. To compensate for the insufficient diversity of tail classes, MBJ re-balances each class with higher sampling probability on tail classes. Specifically, each feature in current mini-batch is sampled into the memory bank according to a certain probability. The probability is class-specific and dependent on the sample volume of each class. MBJ assigns small sampling probabilities to head classes, as well as large sampling probabilities to tail classes, which is formulated as:

$$P_i = \frac{(1/N_i)^\beta}{\sum_i (1/N_i)^\beta} \tag{1}$$

where the N_i is the sample number of the i-th class, P_i is the corresponding sampling probability, and β is a hyper-parameter to control the strength of re-balancing. Intuitively, a larger β results in higher concentration on the tail classes. We use $\beta = 1.5$ in all of our experiments.

To control the memory size, we use a queue strategy for updating the memory bank. After the memory bank reaches its size limitation, we enqueue the newest features with labels, and dequeue the oldest ones. Notably, MBJ only requires a very small memory size to achieve significant improvement.

Given the feature memory along with the batch features, MBJ combines both of them to learn the classifier in a joint optimization manner. Specifically, MBJ uses the features in current mini-batch

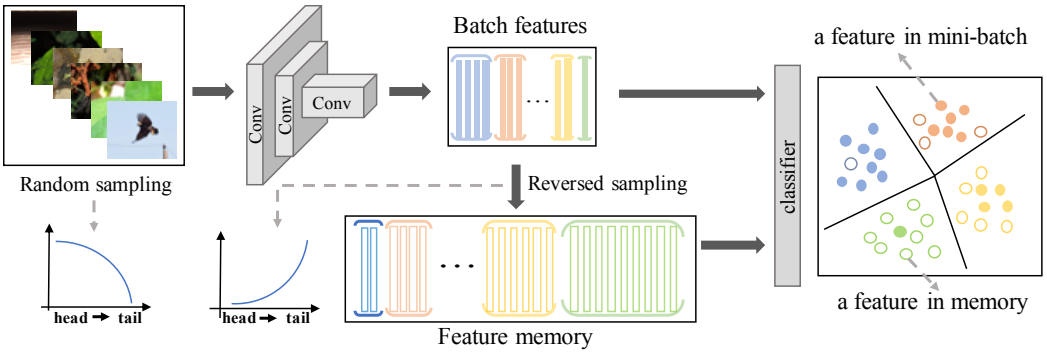

Figure 3: MBJ for image classification collects historical features into memory with higher concentration on tail classes. MBJ randomly samples the raw images and transforms them into a batch of features with a convolutional neural network. Given current batch features, MBJ uses a class-specific sampling strategy to collect the features from different classes. Head classes have smaller sampling probability and tail classes have larger sampling probability. These features are stored into a memory bank, *i.e.*, feature memory. MBJ combines the feature memory and the batch features to learn the classifier. The feature memory compensates the tail classes with higher diversity.

and the weight vectors in the classification layer to deduce a cross-entropy loss, *i.e.*, the loss $\mathcal{L}_{batch}$. Meanwhile, MBJ uses the memorized features and the weight vectors in the classification layer to deduce another cross-entropy loss, *i.e.*, the loss $\mathcal{L}_{memory}$. We note that $\mathcal{L}_{memory}$ only have gradients back-propagated to the weight vectors, because the memorized features do NOT require to be updated by back-propagation. In another word, the memorized features remain unchanged until they are dequeued from the memory bank. Given the batch loss $\mathcal{L}_{batch}$ and the memory loss $\mathcal{L}_{memory}$, MBJ simply sums them up by:

$$\mathcal{L}_{total} = \mathcal{L}_{memory} \times \eta + \mathcal{L}_{batch}, \tag{2}$$

in which η is a weighting factor.

3.3 Deep metric learning

A popular baseline [22, 19, 28, 26, 21, 29, 30] for deep metric learning is as follows: during training, we learn a classification model on the training set. During testing, the distance between two images are measured under the learned deep embedding. To improve deep metric learning on long-tailed data, MBJ shifts its emphasis from tail feature augmentation (as in Section 3.2) to tail prototype augmentation. Specifically, the weight vectors in the classification layer are typically recognized as prototypes for each class. These prototypes also present jitters during training. MBJ collects the historical prototypes to form a prototype memory with higher concentration on the tail classes.

The re-balancing strategy is exactly the same as that in classification. So we omit the detailed description. Given the prototypes in memory and the up-to-date prototypes, MBJ combines both to learn the features. For a specified feature x in current mini-batch, we denote the corresponding prototypes in memory as m and the corresponding up-to-date prototypes as w. In Eq.3 and Eq.4, we use the subscripts p and n to mark the prototypes that is the same class as x and the different class from x respectively.

We use a popular loss function , *i.e.*, CosFace [38], to learn with the up-to-date prototypes, which is formulated by:

$$\mathcal{L}_{batch} = \log\left(1 + \sum_{k=1}^{C-1} \exp\left(\alpha(xw_n^k + \delta - xw_p)\right)\right) \tag{3}$$

in which C is the number of class, α is a scale factor and δ is a margin for better similarity separation.

In the prototype memory, there may be multiple prototypes for each class in memory bank. Some canonical classification losses [27, 20, 37, 38, 36, 7] do not accommodate multiple prototypes per class.

We find that Circle Loss[28] provides an unified loss, which allows multiple similarities associated with a single sample feature. Given a sample features x, let us assume there are P positive prototypes (*i.e.*, prototypes for the target class of x), and N negative prototypes (*i.e.*, prototypes for the non-target class). We modify Circle Loss to learn from the prototype memory by:

$$\mathcal{L}_{memory} = \log\Big(1 + \sum_{j=1}^{N} \exp\big(\alpha(xm_n^j + \delta)\big) \sum_{i=1}^{P} \exp\big(-\alpha(xm_p^i)\big)\Big) \tag{4}$$

Similar to classification, MBJ sums the two types of loss by Eq.2 in deep metric learning. We note that two editions of MBJ share most of implementation details, except for the objects to be memorized (and the corresponding loss). To improve the classification accuracy, MBJ memorizes the historical embeddings; To improve the retrieval accuracy, MBJ memorizes the historical prototypes. These two editions of MBJ have a dual pattern against each other (as to be detailed in Section 4.4).

4 Experiments

Section 4.2 and Section 4.3 evaluate MBJ under image classification task and deep metric learning task, respectively. Section 4.4 conducts ablation study to show that MBJ favors feature memory for classification and prototype memory for deep metric learning, respectively.

4.1 Datasets and setup

Classification task. Inaturalist18 is a large-scale real-world dataset with extremely imbalanced label distribution. It is composed of 437,513 images from 8,142 categories. We adopt the official training and validation splits for our experiments. The original versions of CIFAR-10 and CIFAR-100 contains 50,000 training images and 10,000 validation images of size 32x32 with 10 and 100 classes respectively. Following [5], we create several long-tail version of CIFAR datasets. We use an imbalance ratio ρ to denote the ratio between sample size of the most frequent and least frequent class, *i.e.*, $\rho = \frac{N_{max}}{N_{min}}$, and this imbalance follows an exponential decay in sample sizes across different classes. Imbalanced ratio in our experiments are 10 , 50 and 100, respectively.

Deep metric learning. Market-1501[43] and DukeMTMC-reID[23, 44] are widely used in person re-identification. Following the settings in feature cloud [19], we synthesize several long-tailed editions based on the original datasets. We mark the top H most frequent identities as head classes. The rest are treated as tail classes and the number of samples is reduced to 5 for each tail class (denoted as S5). In our experiments, we set the H to 100, 50 and 20 respectively and form the training sets of <H100,S5>, <H50,S5>, <H20,S5>.

4.2 Experiments on classification

Table 1 compares MBJ with baselines and several state-of-the-art methods. We adopt two baselines, *i.e.*, CE Basel. and the Focal Basel. They are the canonical classification network trained with cross-entropy loss and focal loss [17], respectively. We draw three observations as follows:

First, MBJ significantly improves the baselines on all the three datasets. For example, compared with the cross-entropy baseline, MBJ reduces the error rate by -10.88%, -7.44% and -11.48% on CIFAR-10 (imbalanced ratio 100), CIFAR-100 (imbalanced ratio 100) and iNaturalist18, respectively. Second, comparing MBJ with state-of-the-art methods, we find that MBJ achieves competitive accuracy. On CIFAR-10 (imbalanced ratio 100), the error rate of MBJ is lower than the second best method BBN by -1.42%. On the large scale dataset iNaturalist18, MBJ achieves 31.36% error rate, which is lower than second best method LDAM-DRW by -0.64%.

Table 1: Comparison with baselines and the state-of-the-art methods on long-tailed CIFAR-10, CIFAR-100 and iNaturalist18. We report top-1 error rates. Best results are in **bold**. IEM* denotes the IEM [48] using global feature for fair comparison.

Dataset	Long-tailed CIFAR-10			Long-tailed CIFAR-100			iNaturalist18
Imbalanced ratio	100	50	10	100	50	10	-
Basel. (CE)	29.64	25.19	13.61	61.68	56.15	44.29	42.84
Basel. (Focal) [17]	29.62	23.28	13.34	61.59	55.68	44.22	-
CB Focal [6]	25.43	20.73	12.90	60.40	54.83	42.01	38.88
LDAM-DRW [5]	22.97	18.97	11.84	57.96	53.38	41.29	32.00
BBN [46]	20.18	17.82	**11.68**	57.44	52.98	40.88	33.71
IEM* [48]	-	-	-	-	-	-	33.00
MBJ	**18.76**	**13.31**	11.96	**54.24**	**47.44**	**38.75**	**31.36**

4.3 Experiments on deep metric learning

We evaluate MBJ under a popular deep metric learning task (re-ID, in particular). We note that the long-tail problem on this task has been noticed very recently, and the competing methods are relatively few. Table 2 compares MBJ with re-ID baseline and a state-of-the-art method (Feature Cloud[19]), from which we draw two observations:

First, under typical long-tailed distribution, MBJ significantly improves the re-ID baseline. When there are only 20 head classes and 5 samples per tail class (<H20,S5>), MBJ achieves $+11.1\%$ and $+10.9\%$ mAP on Market-1501 and DukeMTMC-reID, respectively.

Second, MBJ marginally surpasses the recent state-of-the-art, *i.e.*, Feature Cloud [19]. For example, under three long-tailed condition on Market-1501, MBJ achieves 72.6%, 68.8% and 66.7% mAP, which are higher than Feature Cloud by $+3.9\%$, $+1.5\%$ and $+2.6\%$, respectively.

Many memory bank based methods are implemented using a momentum update to avoid reducing the representations' consistency of the content in memory bank, while MBJ is different from them. In MBJ, we argue that the model jitters stored in memory bank are informative and offer cues to augment tail classes with higher diversity. we apply momentum update for memory bank, the result of which is shown as MBJ* in table 2. We find it considerably deteriorates the performance. For example, under the setting of DukeMTMC-reID <H20,S5>, the mAP and Rank-1 accuracy of MBJ* is 54.4% (-3.5%) and 72.3% (-3.2%), respectively.

Table 2: Evaluation of MBJ on long-tailed re-ID task. We report Rank-1 accuracy (R-1) and mAP on Market-1501 and DukeMTMC-reID. Under each dataset, there are three different long-tail conditions. MBJ* denotes the the memory bank of MBJ is implemented using a momentum update. Best performance are in **bold**.

Dataset →	Market-1501						DukeMTMC-reID					
Method ↓	<H100,S5>		<H50,S5>		<H20,S5>		<H100,S5>		<H50,S5>		<H20,S5>	
	mAP	R-1	mAP	R-1	mAP	R-1	mAP	R-1	mAP	R-1	mAP	R-1
Baseline	62.8	83.8	60.5	80.7	55.6	78.6	52.6	70.3	48.0	67.7	47.0	66.0
Feature cloud [19]	68.7	86.5	67.3	84.9	64.1	83.2	55.6	74.8	53.1	73.0	52.4	72.7
MBJ*	71.2	87.3	67.1	85.1	66.0	84.2	59.4	77.5	54.2	73.2	54.4	72.3
MBJ	**72.6**	**88.4**	**68.8**	**86.2**	**66.7**	**84.8**	**60.8**	**78.6**	**56.7**	**74.4**	**57.9**	**75.5**

4.4 Ablation study

While MBJ shares a uniform underlying mechanism for classification and deep metric learning, it has some task-specific modifications. In Section 3.2, MBJ stores the historical features for classification. In Section 3.3 , MBJ stores the historical prototypes. We explain such modifications with an ablation study. We implement three different editions of MBJ, *i.e.*, MBJ-W (storing prototypes), MBJ-F (storing features) and MBJ-WF (storing both prototypes and features) and investigate their performance in Fig. 4.

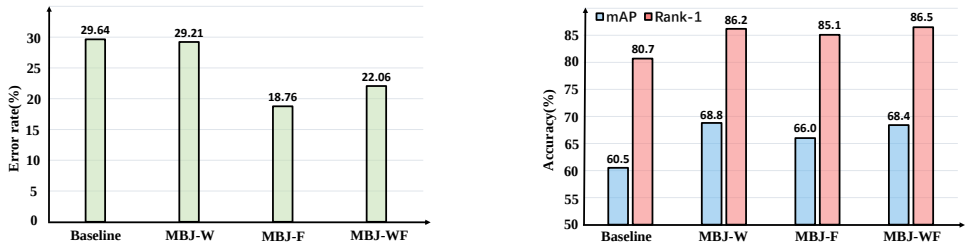

Figure 4: The performance comparison between several variant implementation of MBJ on CIFAR-10(imbalanced ratio 100) and Market-1501(<H50,S5>). In (a), MBJ-F achieves the lowest error rate on classification. In (b), MBJ-W achieves the best performance on deep metric learning, which does not get incremental improvement even combined with MBJ-F.

For classification task, we draw two observations from Fig. 4(a). First, compared with the baseline, MBJ-F significantly reduces the error rate, while MBJ-W barely shows improvement. Second, MBJ-WF is inferior to MBJ-F with +3.3% error rate. It indicates that adding prototype memory actually deteriorates MBJ-F. So we adopts feature memory to implement MBJ for classification task.

For deep metric learning task, we draw three observations from Fig. 4 (b). First, all editions of MBJ significantly improve the re-ID accuracy over the baseline. Second, comparing MBJ-W with MBJ-F, we find that MBJ-W is superior (with +2.8% mAP). Third, comparing MBJ-W with MBJ-WF, we find that adding feature memory to MBJ-W does not bring incremental improvement.

Based on the above investigations, we adopts a respective memory type for these two long-tailed visual recognition tasks, *i.e.*, MBJ-F (feature memory) for classification and MBJ-W (prototype memory) for deep metric learning.

5 Conclusion

This paper proposes Memory-based Jitter (MBJ) to improve long-tailed visual recognition under both deep classification and deep metric learning tasks. The insights behind MBJ are two-fold. First, the model jitters encode the within-class diversity of the overall data and are thus informative. Second, storing these jitters provides extra augmentation for the tail data. Experimental results confirm MBJ significantly improves the baseline and achieves state-of-the-art performance both on image classification and deep metric learning.

An interesting observation is that MBJ favors different types of memory, depending on the specified task. For image classification, it favors the feature memory, while for deep metric learning, it favors the prototype memory. The underlying reasons for such preference are remained to be explored in our future work.

References

[1] Léon Bottou. Large-scale machine learning with stochastic gradient descent. In *Proceedings of COMPSTAT'2010*, pages 177–186. Springer, 2010.

[2] Mateusz Buda, Atsuto Maki, and Maciej A Mazurowski. A systematic study of the class imbalance problem in convolutional neural networks. *Neural Networks*, 106:249–259, 2018.

[3] Mateusz Buda, Atsuto Maki, and Maciej A Mazurowski. A systematic study of the class imbalance problem in convolutional neural networks. *Neural Networks*, 106:249–259, 2018.

[4] Jonathon Byrd and Zachary Lipton. What is the effect of importance weighting in deep learning? In *International Conference on Machine Learning*, pages 872–881, 2019.

[5] Kaidi Cao, Colin Wei, Adrien Gaidon, Nikos Arechiga, and Tengyu Ma. Learning imbalanced datasets with label-distribution-aware margin loss. In *Advances in Neural Information Processing Systems*, pages 1565–1576, 2019.

[6] Yin Cui, Menglin Jia, Tsung-Yi Lin, Yang Song, and Serge Belongie. Class-balanced loss based on effective number of samples. In *CVPR*, pages 9268–9277, 2019.

[7] Jiankang Deng, Jia Guo, Niannan Xue, and Stefanos Zafeiriou. Arcface: Additive angular margin loss for deep face recognition. In *Proceedings of the IEEE Conference on Computer Vision and Pattern Recognition*, pages 4690–4699, 2019.

[8] Mark Everingham, Luc Van Gool, Christopher KI Williams, John Winn, and Andrew Zisserman. The pascal visual object classes (voc) challenge. *International journal of computer vision*, 88(2):303–338, 2010.

[9] Priya Goyal, Piotr Dollár, Ross Girshick, Pieter Noordhuis, Lukasz Wesolowski, Aapo Kyrola, Andrew Tulloch, Yangqing Jia, and Kaiming He. Accurate, large minibatch sgd: Training imagenet in 1 hour. *arXiv preprint arXiv:1706.02677*, 2017.

[10] Yandong Guo, Lei Zhang, Yuxiao Hu, Xiaodong He, and Jianfeng Gao. Ms-celeb-1m: A dataset and benchmark for large-scale face recognition. In *European conference on computer vision*, pages 87–102. Springer, 2016.

[11] Kaiming He, Haoqi Fan, Yuxin Wu, Saining Xie, and Ross Girshick. Momentum contrast for unsupervised visual representation learning. *arXiv preprint arXiv:1911.05722*, 2019.

[12] Kaiming He, Xiangyu Zhang, Shaoqing Ren, and Jian Sun. Deep residual learning for image recognition. In *Proceedings of the IEEE conference on computer vision and pattern recognition*, pages 770–778, 2016.

[13] Chen Huang, Yining Li, Chen Change Loy, and Xiaoou Tang. Learning deep representation for imbalanced classification. In *CVPR*, pages 5375–5384, 2016.

[14] Bingyi Kang, Saining Xie, Marcus Rohrbach, Zhicheng Yan, Albert Gordo, Jiashi Feng, and Yannis Kalantidis. Decoupling representation and classifier for long-tailed recognition. *arXiv preprint arXiv:1910.09217*, 2019.

[15] Alex Krizhevsky, Geoffrey Hinton, et al. Learning multiple layers of features from tiny images. 2009.

[16] Samuli Laine and Timo Aila. Temporal ensembling for semi-supervised learning. *arXiv preprint arXiv:1610.02242*, 2016.

[17] Tsung-Yi Lin, Priya Goyal, Ross Girshick, Kaiming He, and Piotr Dollár. Focal loss for dense object detection. In *Proceedings of the IEEE international conference on computer vision*, pages 2980–2988, 2017.

[18] Tsung-Yi Lin, Michael Maire, Serge Belongie, James Hays, Pietro Perona, Deva Ramanan, Piotr Dollár, and C Lawrence Zitnick. Microsoft coco: Common objects in context. In *European conference on computer vision*, pages 740–755. Springer, 2014.

[19] Jialun Liu, Yifan Sun, Chuchu Han, Zhaopeng Dou, and Wenhui Li. Deep representation learning on long-tailed data: A learnable embedding augmentation perspective. *arXiv preprint arXiv:2002.10826*, 2020.

[20] Weiyang Liu, Yandong Wen, Zhiding Yu, and Meng Yang. Large-margin softmax loss for convolutional neural networks. In *ICML*, volume 2, page 7, 2016.

[21] Xiaofeng Liu, B. V. K. Vijaya Kumar, Jane You, and Ping Jia. Adaptive deep metric learning for identity-aware facial expression recognition. In *The IEEE Conference on Computer Vision and Pattern Recognition (CVPR) Workshops*, July 2017.

[22] Qi Qian, Lei Shang, Baigui Sun, Juhua Hu, Hao Li, and Rong Jin. Softtriple loss: Deep metric learning without triplet sampling. In *Proceedings of the IEEE International Conference on Computer Vision*, pages 6450–6458, 2019.

[23] Ergys Ristani, Francesco Solera, Roger Zou, Rita Cucchiara, and Carlo Tomasi. Performance measures and a data set for multi-target, multi-camera tracking. In *European Conference on Computer Vision*, pages 17–35. Springer, 2016.

[24] Adam Santoro, Sergey Bartunov, Matthew Botvinick, Daan Wierstra, and Timothy Lillicrap. Meta-learning with memory-augmented neural networks. In *International conference on machine learning*, pages 1842–1850, 2016.

[25] Li Shen, Zhouchen Lin, and Qingming Huang. Relay backpropagation for effective learning of deep convolutional neural networks. In *ECCV*, pages 467–482, 2016.

[26] Kihyuk Sohn. Improved deep metric learning with multi-class n-pair loss objective. In D. D. Lee, M. Sugiyama, U. V. Luxburg, I. Guyon, and R. Garnett, editors, *Advances in Neural Information Processing Systems 29*, pages 1857–1865. Curran Associates, Inc., 2016.

[27] Yi Sun, Xiaogang Wang, and Xiaoou Tang. Deep learning face representation from predicting 10,000 classes. In *Proceedings of the IEEE conference on computer vision and pattern recognition*, pages 1891–1898, 2014.

[28] Yifan Sun, Changmao Cheng, Yuhan Zhang, Chi Zhang, Liang Zheng, Zhongdao Wang, and Yichen Wei. Circle loss: A unified perspective of pair similarity optimization. *arXiv preprint arXiv:2002.10857*, 2020.

[29] Yifan Sun, Liang Zheng, Weijian Deng, and Shengjin Wang. Svdnet for pedestrian retrieval. In *Proceedings of the IEEE International Conference on Computer Vision*, pages 3800–3808, 2017.

[30] Yifan Sun, Liang Zheng, Yi Yang, Qi Tian, and Shengjin Wang. Beyond part models: Person retrieval with refined part pooling (and a strong convolutional baseline). In *Proceedings of the European Conference on Computer Vision (ECCV)*, pages 480–496, 2018.

[31] Antti Tarvainen and Harri Valpola. Mean teachers are better role models: Weight-averaged consistency targets improve semi-supervised deep learning results. In *Advances in neural information processing systems*, pages 1195–1204, 2017.

[32] Bart Thomee, David A. Shamma, Gerald Friedland, Benjamin Elizalde, Karl Ni, Douglas Poland, Damian Borth, and Li-Jia Li. Yfcc100m: The new data in multimedia research. *Commun. ACM*, 59(2):64–73, January 2016.

[33] Antonio Torralba, Rob Fergus, and William T Freeman. 80 million tiny images: A large data set for nonparametric object and scene recognition. *IEEE transactions on pattern analysis and machine intelligence*, 30(11):1958–1970, 2008.

[34] Grant Van Horn, Oisin Mac Aodha, Yang Song, Yin Cui, Chen Sun, Alex Shepard, Hartwig Adam, Pietro Perona, and Serge Belongie. The inaturalist species classification and detection dataset. In *Proceedings of the IEEE conference on computer vision and pattern recognition*, pages 8769–8778, 2018.

[35] Grant Van Horn and Pietro Perona. The devil is in the tails: Fine-grained classification in the wild. *arXiv preprint arXiv:1709.01450*, 2017.

[36] Feng Wang, Jian Cheng, Weiyang Liu, and Haijun Liu. Additive margin softmax for face verification. *IEEE Signal Processing Letters*, 25(7):926–930, 2018.

[37] Feng Wang, Xiang Xiang, Jian Cheng, and Alan Loddon Yuille. Normface: L2 hypersphere embedding for face verification. In *Proceedings of the 25th ACM international conference on Multimedia*, pages 1041–1049, 2017.

[38] Hao Wang, Yitong Wang, Zheng Zhou, Xing Ji, Dihong Gong, Jingchao Zhou, Zhifeng Li, and Wei Liu. Cosface: Large margin cosine loss for deep face recognition. In *Proceedings of the IEEE Conference on Computer Vision and Pattern Recognition*, pages 5265–5274, 2018.

[39] Hao Wang, Yitong Wang, Zheng Zhou, Xing Ji, Dihong Gong, Jingchao Zhou, Zhifeng Li, and Wei Liu. Cosface: Large margin cosine loss for deep face recognition. In *Proceedings of the IEEE Conference on Computer Vision and Pattern Recognition*, pages 5265–5274, 2018.

[40] Xun Wang, Haozhi Zhang, Weilin Huang, and Matthew R Scott. Cross-batch memory for embedding learning. *arXiv preprint arXiv:1912.06798*, 2019.

[41] Yu-Xiong Wang, Deva Ramanan, and Martial Hebert. Learning to model the tail. In *NeurIPS*, pages 7029–7039, 2017.

[42] Xi Yin, Xiang Yu, Kihyuk Sohn, Xiaoming Liu, and Manmohan Chandraker. Feature transfer learning for face recognition with under-represented data. In *Proceedings of the IEEE Conference on Computer Vision and Pattern Recognition*, pages 5704–5713, 2019.

[43] Liang Zheng, Liyue Shen, Lu Tian, Shengjin Wang, Jingdong Wang, and Qi Tian. Scalable person re-identification: A benchmark. In *Proceedings of the IEEE international conference on computer vision*, pages 1116–1124, 2015.

[44] Zhedong Zheng, Liang Zheng, and Yi Yang. Unlabeled samples generated by gan improve the person re-identification baseline in vitro. In *Proceedings of the IEEE International Conference on Computer Vision*, pages 3754–3762, 2017.

[45] Q Zhong, C Li, Y Zhang, H Sun, S Yang, D Xie, and S Pu. Towards good practices for recognition & detection. In *CVPR workshops*, volume 1, 2016.

[46] Boyan Zhou, Quan Cui, Xiu-Shen Wei, and Zhao-Min Chen. Bbn: Bilateral-branch network with cumulative learning for long-tailed visual recognition. *arXiv preprint arXiv:1912.02413*, 2019.

[47] Linchao Zhu and Yi Yang. Compound memory networks for few-shot video classification. In *Proceedings of the European Conference on Computer Vision (ECCV)*, pages 751–766, 2018.

[48] Linchao Zhu and Yi Yang. Inflated episodic memory with region self-attention for long-tailed visual recognition. 2020.

Appendix

A More Details on Deep Metric Learning

As shown in Fig.5, Memory-based Jitter (MBJ) for deep metric learning collects historical prototypes, *i.e.*, the classifier weight vectors, into the memory with higher concentration on tail classes. Specifically, each prototype in current classifier is sampled into the memory bank according to a certain probability. The probability is class-specific and dependent on the sample volume of each class. MBJ assigns small sampling probabilities to head classes, as well as large sampling probabilities to tail classes, which is formulated as:

$$P_i = \frac{(1/N_i)^\beta}{\sum_i (1/N_i)^\beta} \tag{5}$$

where N_i is the sample number of the i-th class, P_i is the corresponding sampling probability, and β is a hyper-parameter to control the strength of re-balancing. Intuitively, a large β results in high concentration on the tail classes. We set β to 1.5 in deep metric learning task.

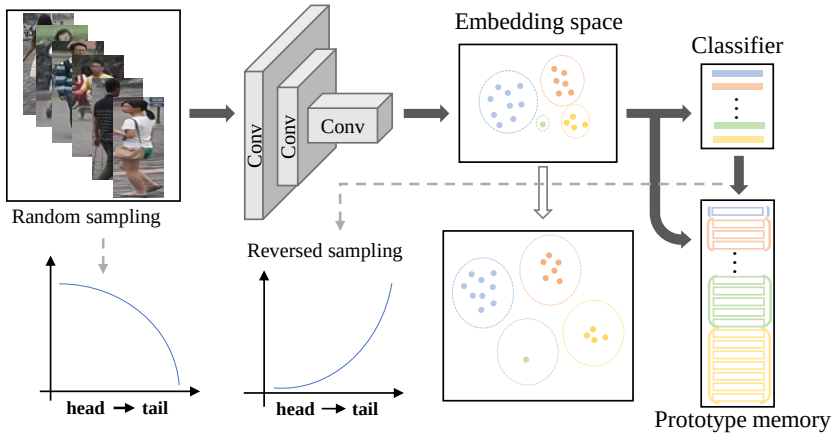

Figure 5: MBJ for deep metric learning collects historical prototypes into memory with higher concentration on tail classes. MBJ randomly samples the raw images and transforms them into a batch of features in embedding space with a convolutional neural network. MBJ uses a class-specific sampling strategy to collect the prototypes, *i.e.*, the classifier weight vectors, from different classes. Head classes have small sampling probability and tail classes have large sampling probability. These prototypes are stored into a memory bank, *i.e.*, prototype memory. MBJ combines the prototype memory and the classifier to learn the embeddings. The prototype memory compensates the tail classes with higher diversity.

B Implementation Details

Implementation details on CIFAR. For long-tailed CIFAR-10 and CIFAR-100 datasets, following the data augmentation strategies proposed in [12], we randomly pad the images with 4 pixels on each side, crop a 32×32 patch and flip it horizontally with a probability of 0.5. In all experiments, we use ResNet32[12] as our backbone network and use stochastic gradient descend with momentum of 0.9, weighting decay of 2×10^{-4} for training. The model is trained with a mini-batch size of 32 for 200 epochs on a single GPU. The initial learning rate is set at 0.1 and decayed by 0.01 at the 120th and 160th epoch respectively. The first five epoch is trained with the linear warm-up learning rate schedule [9]. For the experiments on CIFAR, the hyper-parameters are set as follows: The loss ratio η (Eq. 2) is set to 15. The memory size is set to 500. The re-balancing factor β (Eq. 5) is set to 1.5.

Implementation details on iNaturalist18. We follow the same training strategies in [9] with batch size of 128 on four GPUs. The image is resized by setting the shorter side to 256 pixels, and then we randomly crop a 224×224 patch from it or its horizontal flip. The backbone network we use is ResNet-50[12]. We train the network for 180 epochs with an initial learning rate of 0.01, which is

decayed by 0.1 at the 120th and 160th epoch. The first five epoch is trained with the linear warm-up learning rate schedule [9]. For the experiments on iNaturalist18, the hyper-parameters are set as follows: The loss ratio η (Eq. 2) is set to 15. The memory size is set to 25000. The re-balancing factor β (Eq. 5) is set to 1.5.

Implementation details on person re-identification. We adopt ResNet50 [12] as our backbone network. The last layer of network is followed by a Batch Normalization layer. The Adam optimizer is adopted to optimize the model. We train the model for 120 epoch with batch size of 64. The initial learning rate is set to be 3.5×10^{-4} and is decayed by 0.1 at the 40th epoch and 70th epoch respectively. We use CosFace[39] as the loss function. The scaling factor and margin of CosFace are set to 16 and 0.2, respectively. For the experiments on person re-identification, the hyper-parameters are set as follows: The loss ratio η (Eq. 2) is set to $1/7$. The memory size is set to 3500. The re-balancing factor β (Eq. 5) is set to 1.5.

C Additional Ablation Study

In MBJ, the model jitters provide higher diversity for tail data and thus improve visual recognition on long-tailed data. We wonder whether the model jitters benefit visual tasks on balanced data as well. To this end, we use MBJ on standard CIFAR-10 and Market-1501. The results are shown in Table 3, from which we observe that MBJ does not bring any improvement over the baseline. It indicates that the model jitters are informative only for augmenting the tail data, rather than the balanced data. It is consistent with the motivation of our work.

Table 3: MBJ does not improve the baseline on balanced data (the standard CIFAR-10 and the original Market-1501). We report Rank-1 accuracy (R-1) and mAP on Market-1501, and top-1 error rate on CIFAR-10.

Dataset→	CIFAR-10	Market-1501	
Methods↓	Error rate	mAP	R-1
Baseline	7.12	82.7	93.3
MBJ	7.23	83.0	93.3

In Table 4 and 5, we provide the performance of MBJ on tail, medium and head classes of CIFAR-10/100 (imbalanced ratio 100) and iNaturalist18. We find that on CIFAR-10/100, compared with baseline, MBJ deteriorate the performance of head and medium classes, but the performance of tail class is greatly improved. the overall error rate of CIFAR-10 and CIFAR-100 significantly drops 10.87 and 7.44, respectively . On iNaturalist18, the error rate of head, medium and tail classes drops consistently. Cpmpared with baseline, the overall error rate drops 11.48.

Table 4: Error rates of head classes, medium classes and tail classes on CIFAR-10 and CIFAR-100 long-tailed datasets.

Dataset	CIFAR-10 (imbalanced ratio 100)				CIFAR-100 (imbalanced ratio 100)			
	head	medium	tail	overall	head	medium	tail	overall
Baseline	4.50	26.79	38.96	29.63	25.80	43.50	79.70	61.68
MBJ	7.55	27.50	19.58	18.76	32.00	47.05	64.05	54.24

Table 5: Error rates of head classes, medium classes and tail classes on iNaturalist18.

Dataset	iNaturalist18			
	head	medium	tail	overall
baseline	33.63	39.96	46.87	42.84
MBJ	30.20	31.99	31.53	31.36